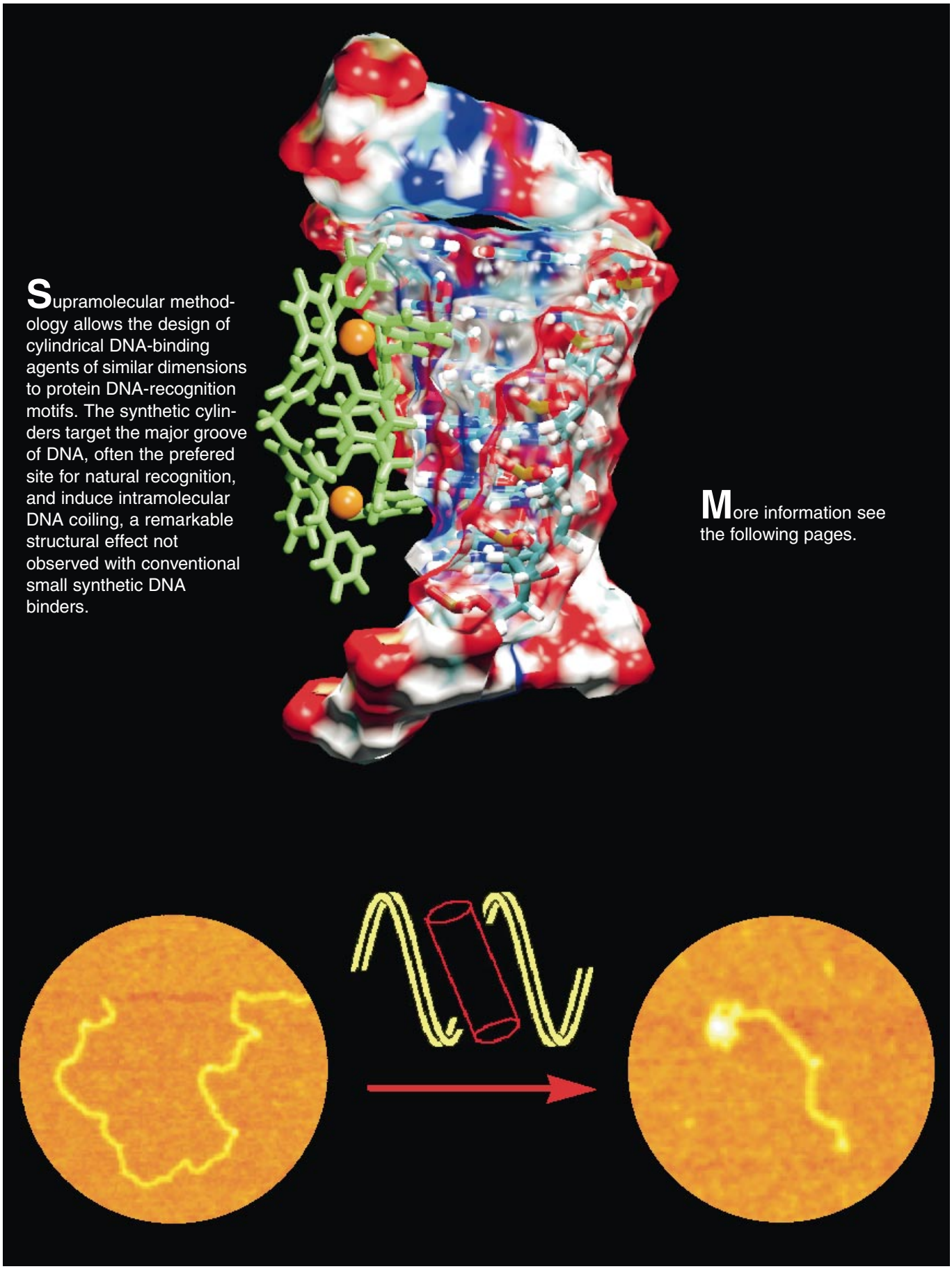

  1433-7851/01/4005-0879 $ 17.50+.50/0

Intramolecular DNA Coiling Mediated by a Metallo-Supramolecular Cylinder**

Michael J. Hannon,* Virtudes Moreno,*
Maria J. Prieto, Erlend Moldrheim, Einar Sletten,*
Isabelle Meistermann, Christian J. Isaac,
Karen J. Sanders, and Alison Rodger*

While DNA encodes the essential blueprint for life, within biological systems its structure and function is regulated by proteins. These macromolecules frequently achieve DNA recognition by binding in or around its major groove since the size and shape of the major groove of B-DNA varies most with base sequence. For example, transcriptional regulators often involve cylindrical binding units, such as alpha helices or zinc fingers, that insert into the major groove and may bend or kink the DNA.[1, 2] Such protein recognition of DNA contrasts with synthetic small-molecule recognition agents, which being smaller than proteins, tend to target the minor groove[3] or act by intercalation[4] and often cause little or no bending of the DNA. Some small polycations, such as spermine, do cause significant DNA bending, resulting in *inter*molecular DNA toroids[5] (this interaction may involve a major-groove component[6]). By way of contrast, in cells, DNA forms tightly compacted *intra*molecular nucleosome core particles by looping, in a series of kinks,[7] around cationic histone proteins.[8] We have designed a metallo-supramolecular cylinder[9, 10] whose size and shape is comparable with a protein zinc finger and herein report a quite unexpected result: that these cylindrical units "wrap up" individual DNA duplexes in an *intra*molecular fashion, which is unprecedented with traditional small-molecule DNA condensation agents.

Supramolecular chemistry provides methodology for the design of large synthetic arrays. We reasoned that supramolecular assembly would allow us to bridge, synthetically, the size gap between traditional small-molecule and larger biomolecule DNA-recognition motifs. We have recently described how synthetic tetracationic supramolecular cylinders (with a triple helical architecture) may be readily prepared through interaction of metal ions with imine-based ligands ($[M_2L_3]^{2n+}$, where n is the charge on each metal, Figure 1).[9, 10] Modelling indicated that these cylinders are the correct size and shape to fit into the B-DNA major groove spanning five base pairs (bp), but are too large to bind in the minor groove (analogous to protein major-groove recognition motifs[2]). Because of their dimetallic nature, the cylinders also have a high positive charge that should enhance their binding to the negatively charged DNA. We have therefore probed the binding of these supramolecular cylinders to DNA.[11]

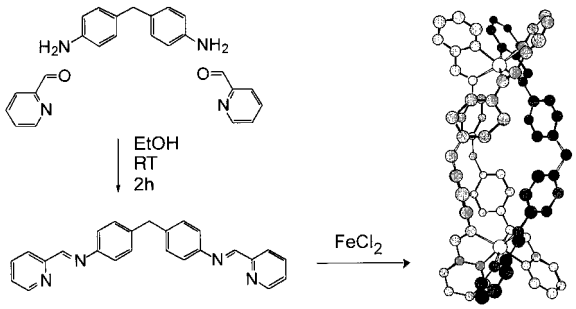

Figure 1. The molecular structure of the ligand and the tetracationic triple helical supramolecular cylinder $[Fe_2(C_{25}H_{20}N_4)_3]Cl_4$.

Circular dichroism (CD, the difference in absorption of left and right circularly polarized light) is sensitive only to the asymmetry or chirality of a system.[12] Thus, with racemic $[Fe_2L_3]^{4+}$ in the presence of DNA, the observation of a CD signal in the optical transitions of $[Fe_2L_3]^{4+}$ indicates that it is binding to the DNA. The induced CD (ICD) spectra (Figure 2b) show that $[Fe_2L_3]^{4+}$ is interacting with the DNA in a single binding mode, which is consistent with major groove binding, when the ligand concentration is below a DNA–bp:cylinder ratio of ~5:1. Above this concentration a change in behavior is observed.[22] The DNA-region CD spectrum is not perturbed significantly at low cylinder loadings suggesting that the DNA geometry is not significantly perturbed. As DNA CD is dominated by local interactions of the bases[12] this implies that any structural perturbations induced by the cylinders do not displace the ligands significantly from their nearest neighbor relative orientations.

Long polymers, such as DNA, can be oriented by the viscous drag created by the rotation of one cylinder inside another. The extent of orientation may be assessed using linear dichroism (LD, the difference in absorption of light polarized parallel and perpendicular to an orientation axis).[12, 13] B-DNA base pairs are oriented approximately perpendicular to the DNA helix axis,[14] which is also the orientation axis, and thus the base $\pi-\pi^*$ transitions give a negative LD signal. If a molecule is bound to DNA in a specific orientation, it will also be oriented by the viscous drag and so exhibit LD signals. If the molecule is free/unbound or bound in a random orientation, then no LD signal is observed for its transitions. For both the low and high loadings of the supramolecular cylinder on DNA, an $[Fe_2L_3]^{4+}$ LD signal is

[*] Dr. M. J. Hannon, Dr. A. Rodger, I. Meistermann,
Dr. C. J. Isaac, Dr. K. J. Sanders
Department of Chemistry
University of Warwick
Coventry, CV4 7AL (UK)
Fax: (+44) 24-76-524112
E-mail: m.j.hannon@warwick.ac.uk, a.rodger@warwick.ac.uk
Prof. V. Moreno, Dr. M. J. Prieto
Departament de Química Inorgànica
Universitat de Barcelona
Diagonal 647, 08028-Barcelona (Spain)
Fax: (+34) 93-490-7725
E-mail: Vmoreno@kripto.qui.ub.es
Prof. E. Sletten, E. Moldrheim
Department of Chemistry
University of Bergen
Allegt 41, 5007 Bergen (Norway)
Fax: (+47) 55-589-490
E-mail: Einar.sletten@kj.uib.no

[**] Support by the Leverhulme Trust (F/215/BC) and the EPSRC lifesciences interface network (GR/M91105) is gratefully acknowledged. Discussions with Julie MacPherson have been of great assistance during preparation of the manuscript.

Supporting information for this article is available on the WWW under http://www.angewandte.com or from the author.

  1433-7851/01/4005-0880 $ 17.50+.50/0

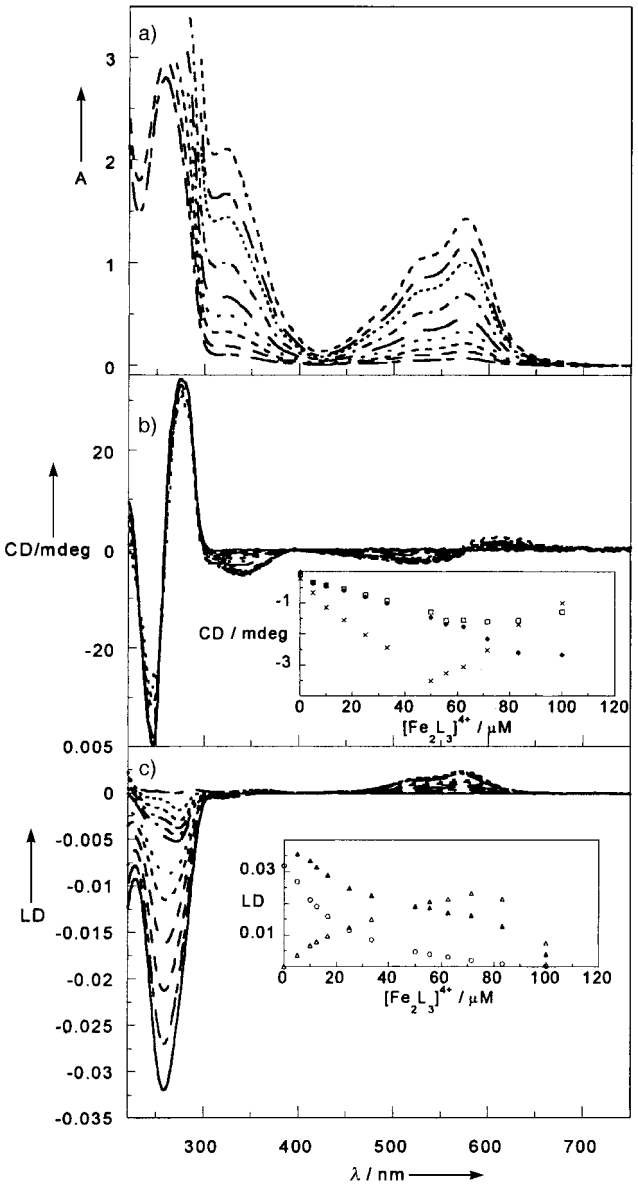

Figure 2. a) Absorbance (1 cm pathlength), b) CD (1 cm pathlength), and c) LD (1 mm pathlength) of 500 μM (in bases) calf thymus DNA (Sigma) in 20 mM NaCl and 1 mM $Na(CH_2)_2AsO_2 \cdot 3H_2O$ buffer (pH 6.8) with increasing concentrations of $[Fe_2L_3]^{4+}$. The DNA base:$[Fe_2L_3]^{4+}$ ratios are for smallest magnitude spectra to largest at 550 nm: 2.5:1, 3:1, 3.5:1, 4:1, 4.5:1, 5:1, 7.5:1, 10:1, 15:1, 25:1, and 50:1. Inserts show CD or LD at key wavelengths as a function of $[Fe_2L_3]^{4+}$ concentration. Insert wavelengths are: × CD at 315 nm; □ CD at 375 nm; ◆ CD at 541 nm; ○ – LD at 258 nm; △ 10 × LD at 568.5 nm; ▲ 500 × LD divided by $[Fe_2L_3]^{4+}$ concentration at 568.5. The 568 nm LD data divided by the $[Fe_2L_3]^{4+}$ concentration is shown to illustrate the different orientations of the cylinder-bound DNA and the average DNA. The solid line corresponds to DNA without any $[Fe_2L_3]^{4+}$.

observed (Figure 2c), confirming its DNA-binding is not random. More importantly, the DNA LD signal arising from the bases is significantly reduced on addition of even very low concentrations of the supramolecular cylinder (at these loadings the 260 nm LD signal can be completely ascribed to the DNA LD). This could result from either an increase in DNA flexibility or a shortening of the DNA by kinking, bending, compaction, or aggregation. The CD (Figure 2b) confirms that the double-stranded B-DNA structure is retained and that the local structure is not significantly perturbed suggesting that kinking is not the reason for DNA shortening. The insert to Figure 2c shows that the 580 nm molar $[Fe_2L_3]^{4+}$ LD signal per molecule decreases more slowly than the DNA signal; this is consistent only with shortening of the DNA through bending.

The extent of shortening can be determined empirically and the results are summarized in Table 1. There is a significant reduction in the average DNA length when $[Fe_2L_3]^{4+}$ is present. It is possible then to estimate the bend angles induced per cylinder to achieve this average length reduction (Table 1). Although such bend-angle calculations are only approximate, it is apparent that at low cylinder loading, there is more effect per cylinder than at high loadings. A bend of $45 \pm 15^\circ$ per cylinder may be estimated, with the higher values being at lower cylinder loadings (Table 1).

Table 1. The effective length of DNA and approximate average bend, $<\theta>$, induced per molecule of $[Fe_2L_3]^{4+}$ to achieve the observed shortening of DNA in solution; n is the number of ligands bound per persistence length[20] of DNA to the nearest whole number. The value of n is overestimated by ~ 1 for the higher ligand loads where the persistence length is reduced (see Figure 3). The values in parentheses indicate what would follow for smaller n. Below a bp:cylinder ratio of 7.5:1 the cylinder contributes more than 20% of the absorbance intensity at 258 nm.

Ligand:DNA Ratio	$-LD^r$ (258 nm)[a]	L^{lig}/L^{free}	n	$<\theta>$[b]
1:∞	0.09667	1.00		
1:100	0.08182	0.87	2	60°
1:50	0.06455	0.71	3	55°
1:40	0.05758	0.64	4 (3)	45° (60°)
1:30	0.04879	0.56	5 (4)	40° (50°)
1:20	0.03485	0.41	7 (6)	35° (40°)
1:15	0.02591	0.31	9 (7)	30° (40°)

[a] The relationship between LD signal and B-DNA length for long DNAs has been found empirically to follow the formula[21] $LD^r = \frac{LD}{A} = -\frac{k_1 G}{k_2 + G}$ where A is the absorbance and G, the velocity gradient of the flow cell, is constant in our experiments, $k_1 = 0.42$ for our experiment (from Figure 8 of ref. [21]), and the inverse of $1/k_2$ is proportional to the DNA length. From ref. [21] it therefore follows that $\frac{L^{lig}}{L^{free}} = \frac{1 + \frac{k_1}{LD^{free}}}{1 + \frac{k_1}{LD^{lig}}}$ where L is the length of DNA, and "lig" and "free" denote in the presence and absence of the ligand respectively. [b] θ Is determined by assuming that the DNA bends are additive, so bend the DNA into a planar circle (rather than a zigzag for which L^{lig}/L would be independent of binding ratio). If n is even then $\frac{L^{lig}}{L} = \frac{2}{n}\left(\frac{1}{2} + \cos(q) + \cdots + \cos\left(\frac{n-1}{2}q\right)\right)$, if n is odd then $\frac{L^{lig}}{L} = \frac{2}{n}(\cos\left(\frac{q}{2}\right) + \cdots + \cos((n-1)\frac{q}{2}))$. Thus θ calculated is the minimum bend per molecule.

To obtain a molecular-level picture of the binding, we have acquired atomic force microscopy (AFM) tapping-mode images of the ligand with a "random" sequence linearized plasmid DNA (Figure 3b–d). At low loading the effect of the cylinders appears to be to increase the average bend angle and number of bends in the DNA compared with the free DNA (Figure 3a), thus reducing the inter-bend distance; consistent with the LD experiments there is a fairly uniform distribution of bound cylinders. The most striking feature of the images is the intramolecular coiling of the DNA at moderate cylinder loadings (Figure 3c). A level of cooperativity is apparent in the coiling process, with some fully coiled strands observed in the presence of uncoiled (but bent) DNAs.

  1433-7851/01/4005-0881 $ 17.50+.50/0

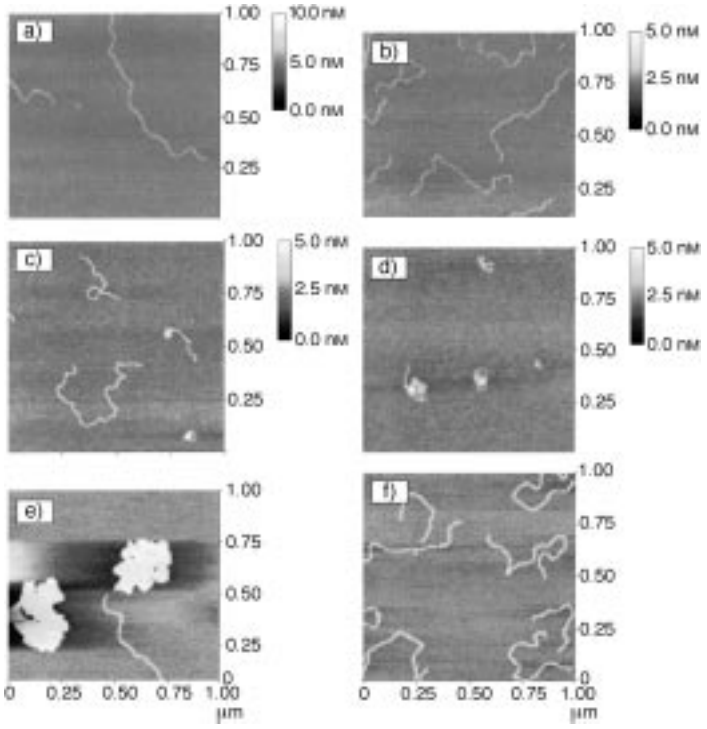

Figure 3. AFM images of linear plasmid DNA (pBR322, 4361 bp, diameter of 475 nm, cleaved with Pst I and Sal I enzymes to give two linear fragments of 1401 bp and 2962 bp) with the following metal complexes (DNA–bp:metal complex ratio given in parentheses): a) free DNA, b) low $[Fe_2L_3]^{4+}$ concentration (10:1), c) medium $[Fe_2L_3]^{4+}$ concentration (10:3), d) high $[Fe_2L_3]^{4+}$ concentration (10:5), e) $[Co(NH_3)_6]^{3+}$, and f) $[Ru(phen)_3]^{2+}$.

AFM images of metal complexes bound to DNA are rare and mainly restricted to the covalent binding of drugs such as *cis*-platin.[15] Therefore to investigate whether these unusual observations were common to AFM images of other non-covalent DNA-binding metal complexes or arose as a result of the larger size, larger charge, and cylindrical shape of our metallo-supramolecular cylinder we analyzed a set of controls under the same conditions. Two well-studied metal complexes with different binding characteristics were selected; $[Co(NH_3)_6]^{3+}$ is a known DNA condensation agent and has been shown by LD to bend DNA.[10] By contrast, $[Ru(phen)_3]^{2+}$ (selected as a "spherical" model for half of $[Fe_2L_3]^{4+}$; phen = 1,10-phenanthroline) does not cause DNA condensation and has comparatively little bending effect, though the Δ enantiomer does reduce the DNA orientation in flow-LD experiments.[16, 17] The cobalt complex condenses and aggregates the DNA into *inter*molecular clusters (Figure 3e). Again the binding appears to be cooperative with clusters observed in the presence of uncoiled DNA strands. With $[Ru(phen)_3]^{2+}$ no *inter* or *intra*molecular packaging was observed, simply an increase in the average size and number of DNA bends (Figure 3f). These images are very similar to those previously reported for $[Ru(phen)_3]^{2+}$ with *p*BluBacHisb DNA.[18] The effect of $[Pt(NH_3)_2Cl_2]$ (*cis*-platin), which covalently binds to DNA mainly in a G–G intrastrand mode that bends the DNA by about 45°,[19] is again distinct from the effect of the cylinder showing larger average bends and shorter links between the bends.

The interaction between a double-helical DNA oligonucleotide, 5′-d(GACGGCCGTC)$_2$, and $[Fe_2L_3]^{4+}$ has also been studied by 1D and 2D NMR spectroscopy to determine the local aspects of the geometry of the binding. A number of nuclear Overhauser enhancement spectroscopy (NOESY) cross-peaks representing contacts between the duplex $[Fe_2L_3]^{4+}$ confirm binding in the major groove (Table 2 and Figure 4).[23] Though this does not preclude other binding

Table 2. Intermolecular NOEs between the helicate and d(GACGGCCGTC)$_2$. The numbering scheme used is illustrated below.

Helicate protons	Chemical shift [ppm]	Nucleic acid protons
S1 H7	8.74	C7B H2′(vw), G5A NH(m), G5A H8(w), C6A NHF(m)
S1 H11	6.25	C6A H5(s), C6A H6(w), C6A NHF(m), C6A NHB(m), G5A NH(m), G5A H8(m)
S1 H13	5.34	C6A H5(m)
S1 H14	4.06	G5A NH(s)
S2 H2	8.33	C6A H2′(w), C6A H2″(m), G5A NH(m)
S2 H3	8.24	C6A H2′(vw), C6A H2″(w), G5A NH(m)
S2 H7	8.84	C6A H2′(w), C6A H2″(m), G5A NH(s), G5A H8(w)
S2 H10	5.19	G4A H3′(w)
S2 H11	6.33	C6A H2′(w), G4A H8(vw), G5A H8(w), G5A NH(m), C6B H5(m), C7B H5(m)
S2 H14	4.28	G5A NH(m)
S3 H2	8.39	G5A NH(m)
S3 H11	6.53	C6B H5(s)
S4 H2	8.32	C7B H2′(w), C7B H2″(m), C6B H6(m), C7B H6(m)
S4 H7	8.53	G5A NH(s), C6B H6(w), C7B H6(w)
S4 H11	6.32	C6B H6(m), C7B H6(m)
S4 H14	3.90	G5A NH(s)

S1–S4, A, and B are defined in the text.

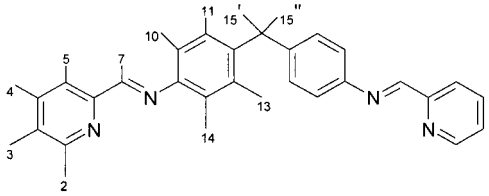

modes at either higher cylinder loadings or that are undetectable by NMR spectroscopy. We observed four different binding positions (in the major groove) of the helicate indicated in Table 2 by S1–S4. The symmetry of the palinodromic oligonucleotide is changed upon addition of the helicate. We observed two sets of signals for the residues C3–G8 (indicated in Table 2 by A and B). When viewed down the groove (third view in Figure 4) contact between $[Fe_2L_3]^{4+}$ and the base of the groove is apparent. The driving force for helix bending observed in the LD and AFM images can easily be envisaged. Nuclear Overhauser effect (NOE) restrained molecular-docking and molecular dynamics calculations are in progress to determine the extent of duplex bending induced by the supramolecular cylinder. Further details of the NMR spectroscopy including NOESY and total correlation spectroscopy (TOCSY) spectra are included in the Supporting Information.

In conclusion, we have shown that supramolecular methodology can be used to design DNA-binding motifs of a similar

  1433-7851/01/4005-0882 $ 17.50+.50/0

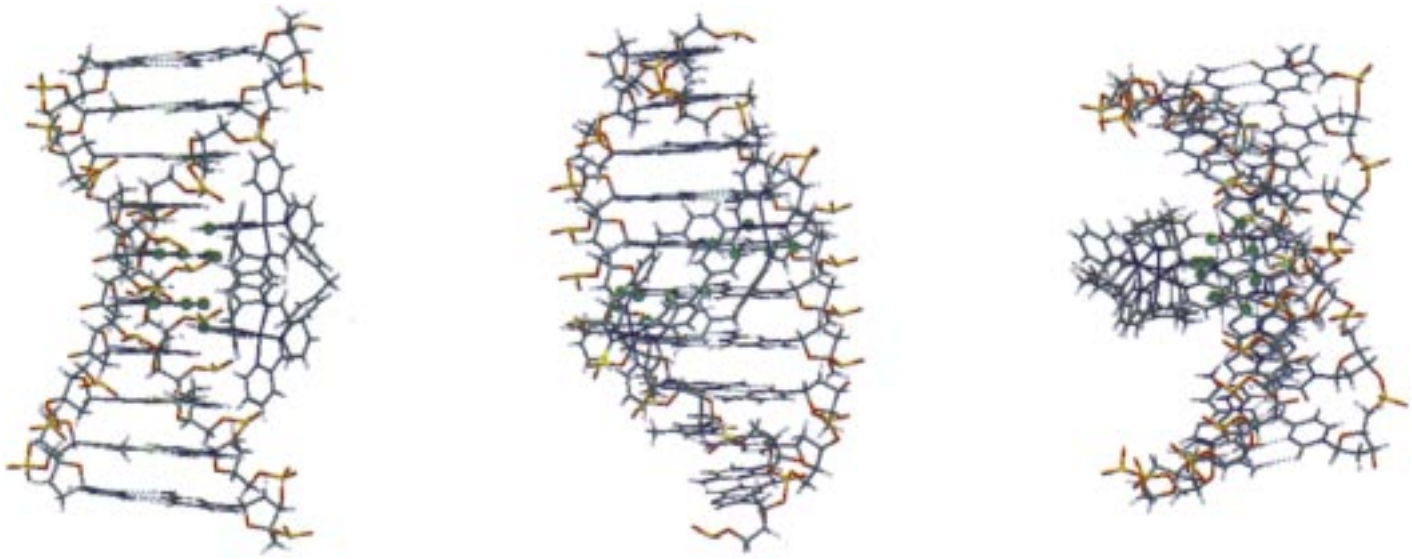

Figure 4. Views of $[Fe_2L_3]^{4+}$ docked into the major groove of [5′-d(GACGGCCGTC)]$_2$ based on NMR experiments. A number of NOESY cross-peaks representing contacts, indicated by circles, between the duplex $[Fe_2L_3]^{4+}$ confirms binding in the major groove.

scale to those found in nature. These large binding motifs can lead to remarkable effects on DNA structure, as observed by CD, LD, and AFM. Intermolecular NOEs between the complex and DNA confirms that the cylinder binds to DNA in the major groove. There may also be other NMR-silent binding modes. We are currently assessing the extent to which this approach can be extended with new supramolecular arrays designed to achieve specific structural effects in a sequence specific fashion. The topic of DNA structure control by proteins, and, by extension, synthetic analogues, is of particular relevance in the light of the ongoing quest to understand not only the coding inherent in DNA, but how it is processed or may be suppressed in biosystems.

Experimental Section

Absorbance spectra were collected using a Jasco V-550 UV/Vis absorption spectrometer. CD and LD spectra were collected using a Jasco J-715 spectropolarimeter adapted for LD measurements. The LD samples were oriented in a radial couvette flow cell.[28]

AFM images of linear plasmid DNA (pBR322, 4361 bp, diameter of 475 nm, cleaved with PstI and SalI enzymes to give two linear fragments of 1401 bp and 2962 bp) were collected with a range of metal complexes. DNA–metal complex adducts were prepared as follows: digested pBR322 DNA (15 ng) was incubated in an appropriate volume with the required metal complex in 2-[4-(2-hydroxyethyl)-1-piperazinyl]ethanesulfonic acid (HEPES) buffer (HEPES 4 mM pH 7.4, KCl 5 mM, and $MgCl_2$ 2 mM). All solutions were made with water (18.2 MΩ) filtered through 0.2 nm FP030/3 filters (Schleicher & Schuell GmbH, Germany) and centrifuged at 4000 g several times to avoid salt deposits and provide a clear background when they were imaged by AFM. The samples were left to equilibrate at 37 °C for 5 h in the dark. Samples were prepared for AFM by placing a drop (6 μL) of DNA solution or DNA–metal complex solution onto Ni-treated green mica (Ashville–Schoonmaker Mica Co., Newport New, VA). After adsorption for five minutes at room temperature, the samples were rinsed for 10 s in a jet of deionized water (18 MΩ cm^{-1} Milli-Q water) directed onto the surface with a squeeze bottle. The samples were blow dried with compressed argon over silica gel and then imaged using a Nanoscope III Multimode AFM (Digital Instrumentals Inc., Santa Barbara, CA) operating in tapping mode in air at a scan rate of 1–3 Hz. The AFM probes were 125 μm-long monocrystalline silicon cantilever with integrated conical shaped Si tips (Nanosensors GmbH, Germany) with an average resonance frequency of 330 kHz and spring constant $K = 50$ N m^{-1}. The cantilever is rectangular and the tip radius given by the supplier is 10 nm with a cone angle of 35° and high aspect ratio. The images were obtained at room temperature ($T = 23 \pm 2$ °C) and typical relative humidity of > 55 %. Four different samples from each reaction were imaged in several places and many times to obtain reliable measurements. The persistence length (the length over which the average deflection of the helix axis is one radian (57.3°)) for each DNA was determined by assuming the DNA is flat on the surface of the mica and converting the segment lengths to base pairs (bp) by dividing by 0.36 nm. This value will be a lower bound as it is a projection of the length onto a plane. The average bend is determined by summing successive bends until a value greater than 57°, then recording the length and bend obtained. This value will be an upper bound because of the projection issue. The values of these average parameters are approximately: 120 bp/67° for free DNA; 92 bp/69° wrapped into intramolecular bundles with $[Fe_2L_3]^{4+}$; 92 bp/70° with $[Ru(phen)_3]^{2+}$; 114 bp/68° condensed with $[Co(NH_3)_6]^{3+}$; and 80 bp/80° with cisplatin.

NMR spectra were recorded on a Bruker DRX 600 MHz instrument using a 2.8 mM sample of the oligonucleotide purchased from Oswel DNA Service. The sample was purified with ion-exchange chromatography, desalted, and paramagnetic impurities were removed using a Chelex column. The oligonucleotide was then dissolved in 90 % H_2O and 10 % D_2O containing 50 mM phosphate buffer and 40 mM NaCl. The pH of the sample was 6.9. $[Fe_2L_3]^{4+}$ was added in five steps to reach a 1:2 ratio. This ratio was selected so that no precipitation should occur. A combination of through space nuclear Overhauser effect (NOESY) and through bond correlated (TOCSY) two-dimensional spectra were recorded. The spectra were recorded at 17 °C using Double Pulsed Field Gradients Spin Echo water suppression (dpfgsew5).[25, 26] The data were processed using XWIN-NMR (Bruker) and analyzed using Sparky.[27] The imino protons were clearly observed indicating that the double-helical geometry was retained. TOCSY experiments were performed to facilitate the assignment procedure and clearly show the double sets of signals for the central residues of the DNA. A number of cross-peaks in the NOESY map represent proton–proton contacts between the oligonucleotide and $[Fe_2L_3]^{4+}$ as shown in Table 2. Molecular docking was performed using the DOCK 4.0.1 suite of programs.[24] A grid was constructed on the basis of the NOE contacts. The grid spacing was 0.2 Å and the sampling size was 10000 structures. The 30 best results were then energy minimized.

Received: October 2, 2000
Revised: December 18, 2000 [Z15889]

  1433-7851/01/4005-0883 $ 17.50+.50/0

[1] R. R. Sinden, *DNA Structure and Function*, Academic Press, San Diego, **1994**.
[2] R. E. Dickerson, *Nucleic Acids Res.* **1998**, *26*, 1906 – 1926.
[3] B. C. Baguley, *Mol. Cell. Biochem.* **1982**, *43*, 167 – 181.
[4] W. A. Denny, *Anticancer Drug Des.* **1989**, *4*, 241 – 263.
[5] V. A. Bloomfield, *Biopolymers* **1991**, *31*, 1471 – 1481.
[6] M. Yuki, V. Grukhim, C. S. Lee, I. S. Haworth, *Arch. Biochem. Biophys.* **1996**, *325*, 39 – 46.
[7] J. E. Morgan, J. W. Blankenship, H. R. Matthews, *Biochemistry* **1987**, *26*, 3643 – 3649.
[8] S. E. Wellman, D. B. Sittman, J. B. Chaires, *Biochemistry* **1994**, *33*, 384 – 388.
[9] M. J. Hannon, C. L. Painting, A. Jackson, J. Hamblin, W. Errington, *Chem. Commun.* **1997**, 1807 – 1808.
[10] A. Rodger, K. J. Sanders, M. J. Hannon, I. Meistermann, A. Parkinson, D. S. Vidler, I. S. Haworth, *Chirality* **2000**, *12*, 221 – 236.
[11] A smaller *double*-helicate has been reported to bind to DNA but its mode of binding was not established. B. Schoentjes, J.-M. Lehn, *Helv. Chim. Acta* **1995**, *78*, 1 – 12.
[12] A. Rodger, B. Nordén, *Circular Dichroism and Linear Dichroism*, Oxford University Press, Oxford, **1997**.
[13] B. Nordén, M. Kubista, T. Kurucsev, *Q. Rev. Biophys.* **1992**, *25*, 51 – 170.
[14] P.-J. Chou, W. C. Johnson, *J. Am. Chem. Soc.* **1993**, *115*, 1205 – 1214.
[15] G. B. Onoa, G. Cervantes, V. Moreno, M. J. Prieto, *Nucleic Acids Res.* **1998**, *26*, 1473 – 1480.
[16] C. Hiort, B. Nordén, A. Rodger, *J. Am. Chem. Soc.* **1990**, *112*, 1971 – 1982.
[17] Z. Coggan, I. S. Haworth, P. J. Bates, A. Robinson, A. Rodger, *Inorg. Chem.* **1999**, *38*, 4486 – 4497.
[18] J. E. Coury, J. R. Anderson, L. McFail-Isom, L. D. Williams, L. A. Bottomley, *J. Am. Chem. Soc.* **1997**, *119*, 3792 – 3796.
[19] U.-M. Ohndorf, M. A. Rould, Q. He, C. O. Pabo, S. J. Lippard, *Nature* **1999**, *399*, 708 – 712.
[20] H. G. Hansma, K. J. Kim, D. E. Laney, R. A. Garcia, M. Argaman, M. J. Allen, S. M. Parsons, *J. Struct. Biol.* **1997**, *119*, 99 – 108.
[21] T. Simonson, M. Kubista, *Biopolymers* **1993**, *33*, 1225 – 1235.
[22] It should be noted that attempts to displace the ligand from DNA with ethidium bromide were unsuccessful indicating a binding constant in excess of $\sim 10^7\,\text{M}^{-1}$ under these conditions.
[23] The integrity of the metallo-cylindrical array and the maintenance of the Fe^{II} oxidation state are confirmed by both the NMR studies and the lack of perturbation to the visible chromophore (a metal to ligand charge transfer (MLCT) band in the UV/Vis spectrum).
[24] T. J. A. Ewing, I. D. Kuntz, *J. Comput. Chem.* **1997**, *18*, 1175 – 1189.
[25] M. Liu, X. Mao, C.Ye, H. Huang, J. K. Nicholson, J. C. Lindon, *J. Magn. Reson.* **1998**, *132*, 125 – 129.
[26] T.-L. Hwang, A. J. Shaka, *J. Magn. Reson. A* **1995**, *112*, 275 – 279.
[27] T. D. Goddard, D. G. Kneller, SPARKY3, University of California, San Francisco.
[28] A. Rodger, *Methods Enzymol.* **1993**, *226*, 232 – 258.

Unique Single-Atom Binding of Pseudohalogeno Ligands to Four Metal Ions Induced by Their Trapping into High-Nuclearity Cages**

Giannis S. Papaefstathiou, Spyros P. Perlepes, Albert Escuer,* Ramon Vicente, Mercé Font-Bardia, and Xavier Solans

High-nuclearity transition metal clusters continue to attract a great deal of interest, partly because of their fascinating physical properties and partly for the beauty and complexity of their structures. An interesting subarea of transition metal cluster chemistry is the small but growing family of molecules that, in their ground states, have unusually large numbers of unpaired electrons. Molecular clusters with very high spin values have been prepared, often by one-pot synthesis, with the highest values to date being $S_T = 51/2$ for the recently reported[1] $Mn_9^{II}Mo_6^{V}$ cyano-bridged system and $S_T \approx 33/2$ for one of the clusters in a compound containing cocrystallized Fe_{17} and Fe_{19} species.[2] The large-spin ground state results from either ferromagnetic (or ferrimagnetic) exchange interactions between the paramagnetic centers and/or topologically frustrated antiferromagnetic interactions.[3] In addition, it has recently become apparent that a fairly large S_T value is a necessary (but not sufficient) requirement for molecules to be able to exhibit the new phenomenon of single-molecule magnetism.[4] The synthesis of new high-spin molecules is thus of interest. However, it is difficult to predict in advance what type of topology and structure will lead to a high-spin cluster and even more difficult to then achieve a rational synthesis of such a species.

In most polynuclear clusters, magnetic exchange interactions are mainly propagated by bridging OH^-, OR^-, O^{2-}, or RCO_2^- ligands, or a combination of two or more of these groups; often these interactions lead to antiferromagnetic coupling. An alternative attractive approach to increase the S_T ground state would be the replacement of one or more of the above-mentioned bridging ligands with other groups that are more prone to ferromagnetic coupling. Herein we describe our preliminary results demonstrating the application of this approach.

[*] Dr. A. Escuer, Dr. R. Vicente
Departament de Química Inorgànica
Universitat de Barcelona
Av. Diagonal 647, 08028-Barcelona (Spain)
Fax: (+34) 93-4907725
E-mail: albert.escuer@qi.ub.es
G. S. Papaefstathiou, Prof. S. P. Perlepes
Department of Chemistry
University of Patras
GR-265 00 Patras (Greece)
Fax: (+30) 61-997118
M. Font-Bardia, Prof. X. Solans
Departament de Cristallografia i Mineralogia
Universitat de Barcelona
Marti Franqués s/n, 08028-Barcelona (Spain)

[**] This work was supported by CICYT (Grant BP96/0163) and the Research Committee of the University of Patras (C. Caratheodory Programme, No 1941).

  1433-7851/01/4005-0884 $ 17.50+.50/0